NATIONAL ADVISORY COMMITTEE FOR AERONAUTICS

TECHNICAL NOTE 2401

TEMPERATURE DISTRIBUTION IN INTERNALLY HEATED WALLS OF HEAT EXCHANGERS WITH NONCIRCULAR FLOW PASSAGES USING COOLANTS WITH VERY LOW PRANDTL NUMBER

By E. R. G. Eckert and George M. Low

Lewis Flight Propulsion Laboratory
Cleveland, Ohio

Washington
July 1951

NATIONAL ADVISORY COMMITTEE FOR AERONAUTICS

TECHNICAL NOTE 2401

TEMPERATURE DISTRIBUTION IN INTERNALLY HEATED WALLS OF HEAT EXCHANGERS WITH NONCIRCULAR FLOW PASSAGES USING COOLANTS WITH VERY LOW PRANDTL NUMBER

By E. R. G. Eckert and George M. Low

SUMMARY

In the walls of heat exchangers that are composed of noncircular passages, the temperature varies in a circumferential direction. A prediction of the magnitude of this variation is necessary in order to detect the places of highest temperature and to determine the operating temperatures admissible for the material of which the heat exchanger is composed.

A method for the determination of the temperature distribution within the coolant and the passage walls for a special type of heat exchanger is presented. The heat exchanger is composed of polygonal flow passages which are heated uniformly by internal heat sources. The Prandtl number of the coolant flowing through the passages is postulated to be so low that the turbulent contribution to the heat flow within the fluid can be neglected. The differential equation describing the heat flow by conduction is solved by the relaxation method. Numerical computations are carried out for a triangular and a rectangular passage shape. The resulting ratio of the temperature differences within the passage walls to the difference of the wall temperature and the fluid bulk temperature is considerably larger than the temperature ratio in similar heat exchangers using a coolant with a Prandtl number in the neighborhood of 1.

INTRODUCTION

The conventional recuperative type of heat exchanger consists of passages for two fluids separated by a heating surface. Heat from an external source is transferred continuously from one fluid to the other through the heating surfaces. In the regenerative type of heat exchanger the two fluids pass alternately through the same passages. During the heating period heat is transferred from a hot fluid to the

passage walls and is stored within the solid wall material. During the cooling period this stored heat is then transferred to a cold fluid passing through the heat exchanger.

The heat exchanger considered in this report is very similar to the regenerative type. It differs from it only by the fact that the heat is generated internally by heat sources located within the passage walls and is transferred to a coolant flowing continuously through the passages. The heat-exchanger passages are formed by a number of plates assembled to form a honeycomb. High temperatures may be anticipated near the corners of the flow passages thus formed. A knowledge of the magnitude of these temperatures is necessary in order to determine the admissible operating temperature of the heat exchanger.

In a previous report (reference 1) the temperature distribution in the walls of similar heat exchangers was studied with the assumption that the coolant consists of a fluid with a Prandtl number in the neighborhood of 1. In the present report, the investigation carried out at the NACA Lewis laboratory, is extended to include coolants with a Prandtl number very much less than 1. The Prandtl number is assumed to be so low that the turbulent contribution to the heat transport within the fluid can be neglected as compared with the conductive contribution.

A knowledge of the velocity distribution within the passages is necessary in order to determine the temperature distribution. A thorough investigation of the flow of water through tubes with noncircular cross sections was made by Nikuradse (references 2 and 3). The velocity profiles obtained in this investigation will be used in the present report.

The analysis presented applies to all passage shapes for which the velocity distribution is known and to all possible configurations of these passage shapes. Solutions are presented, however, only for heat exchangers composed of triangular and rectangular passages. Cross-sectional views of these configurations are shown in figures 1 and 2.

SYMBOLS

The following symbols are used in this report:

A	cross-sectional flow area, (sq ft)
A^*	A/D^2, (dimensionless)

C	internal perimeter of passage, (ft)
c	specific heat, (Btu/(lb)($^{\circ}$F))
D	hydraulic diameter, 4A/C, (ft)
d	distance between parallel plates, (ft)
g	acceleration due to gravity, (ft/sec^2)
k	thermal conductivity of coolant, (Btu/(sec)(ft)($^{\circ}$F))
L	distance measured along passage wall in circumferential direction, (ft)
L*	L/D, (dimensionless)
N	residual value, (dimensionless)
n	coordinate normal to passage wall, (ft)
n*	n/D, (dimensionless)
Pr	Prandtl number, $(\nu\rho cg)/k$, (dimensionless)
p	summation index
R	radial coordinate, (ft)
R*	R/D, (dimensionless)
r	rate of internal heat generation, (Btu/(sec)(cu ft))
s	wall thickness, (ft)
T	temperature, ($^{\circ}$F)
T_B	bulk temperature of coolant, $\frac{1}{\bar{u}A}\int_A u\,T\,dA$, ($^{\circ}$F)
T_w	wall temperature, ($^{\circ}$F)
T*	$T\left(\frac{2k}{rsD}\right)$, (dimensionless)
u,v,w	velocity components in x-, y-, and z-directions, (ft/sec)

$\bar{u}$	mean velocity, $\frac{1}{A}\int_A u\,dA$, (ft/sec)
u^*	$u/\bar{u}$, (dimensionless)
x,y,z	Cartesian coordinates
x^*,y^*,z^*	x/D, y/D, z/D, (dimensionless)
Δ	increment of length, (ft)
Δ^*	Δ/D, (dimensionless)
ϵ	turbulent diffusivity of heat, (sq ft/sec)
ν	kinematic viscosity, (sq ft/sec)
ρ	mass density, $((lb)(sec^2)/ft^4)$
τ	time, (sec)
$\frac{D}{D\tau}$	material derivative, $\left(\frac{\partial}{\partial\tau} + u\frac{\partial}{\partial x} + v\frac{\partial}{\partial y} + w\frac{\partial}{\partial z}\right)$
∇^2	Laplacian operator, $\left(\frac{\partial^2}{\partial x^2} + \frac{\partial^2}{\partial y^2} + \frac{\partial^2}{\partial z^2}\right)$

Subscripts:

c	conditions for equivalent circular tube
m	conditions at center of flow passage

Superscript:

*	dimensionless quantity

ASSUMPTIONS

A number of assumptions are necessary in order to make the problem amenable to solution and to obtain results of a general nature. The following assumptions are in agreement with reality for the applications considered:

1. The Prandtl number of the fluid used as coolant is so small that the heat flow by the turbulent mixing movements can be neglected as compared with the heat flow by conduction. In reality the turbulent contribution to the heat flow is of some importance even in liquid metals used as coolants. Therefore, the calculations presented herein deal with a limiting case. In a previous report (reference 1) analogous calculations were presented for a fluid with a Prandtl number of 1. From the results of reference 1 and the results presented herein, it should be possible to estimate the conditions for any fluid with a small Prandtl number.

2. The passages of the heat exchanger are long enough and the Reynolds number is sufficiently high so that in the cross section investigated the flow is fully developed and turbulent. This means that the velocity profile does not change its shape in the direction of the tube axis.

3. The property values for the coolant are constant. Under this condition the flow is independent of the Prandtl number and has the same characteristics as determined by Nikuradse for water.

4. The rate of heat generation in the walls of the heat exchanger is uniform. Consequently the temperature within the coolant and the walls increases linearly in a downstream direction provided the flow is thermally developed. By extrapolation of results for fluids with Prandtl numbers greater than 1 (reference 4), it is found that for a fluid with a Prandtl number less than 1 the tube length required for thermal development is not greater than the tube length needed for velocity development.

5. The thickness of the passage walls is small as compared with the hydraulic diameter. Consequently the heat conduction within the walls of the heat exchanger will be neglected as compared with the heat conduction within the fluid. Coolants with a low Prandtl number are fluids with a high heat conductivity value. Therefore, in all practical cases the heat conductivity of the wall material is not larger than the heat conductivity of the fluid and the conduction in the wall can be neglected as long as the wall thickness is not too large.

DIFFERENTIAL EQUATIONS DESCRIBING HEAT FLOW WITHIN COOLANT

The flow field within the coolant flowing through the passages is described by the continuity and the momentum equations. The temperature field which is superimposed on this field is given by the energy

equation. As long as the property values of the coolant are independent of temperature and as long as free-convection effects can be neglected, the differential equations describing the flow field are independent of the energy equation. The flow field therefore remains unchanged when a heat flow from the passage walls is added to the fluid and is also independent of the Prandtl number. Measurements of the velocity profiles within noncircular passages which were made by Nikuradse (references 2 and 3) on water therefore describe the flow field for any other fluid. These profiles will be used in this report.

The temperature field within a turbulently flowing coolant is described by the following equation when the temperature rise by internal friction can be neglected:

$$\frac{DT}{D\tau} = \nabla^2 T \left(\frac{k}{\rho c g} + \epsilon \right) \tag{1}$$

The temperatures T in this equation are time mean values and all the contributions of the turbulent mixing processes to the heat flow within the coolant are summarily contained in the term $\epsilon \nabla^2 T$. The first term within the bracket $\left(\frac{k}{\rho c g} \right)$ can be expressed as $\frac{\nu}{Pr}$ by definition of the Prandtl number. It is known that there exists, if any, only a minor dependence of the turbulent diffusivity ϵ on the Prandtl number. Therefore, with decreasing Prandtl number the first term in the bracket of equation (1) becomes more and more important and finally for very small Prandtl numbers the second term $\epsilon \nabla^2 T$ can be neglected as compared with the first term. Thus the differential equation (1) reduces to

$$\frac{DT}{D\tau} = \frac{\nu}{Pr} \nabla^2 T \tag{2}$$

A Cartesian coordinate system may be arranged within the flow passage in such a way that the x-axis is parallel to the axis of the passage and normal to the plane of the drawing in figures 1 and 2. The y- and z-axes therefore lie within a cross section of the passage. In fully developed flow only velocity components in the x-direction are present. (The velocities connected with the secondary flow detected by Nikuradse and described in reference 1 are small as compared with the axial velocities.) Under this condition the derivative $\frac{DT}{D\tau}$ is, for steady state, equal to $u \frac{\partial T}{\partial x}$. The gradient $\frac{\partial T}{\partial x}$ is a constant according to assumption 4. Therefore, equation (2) may be written as

$$\frac{Pr}{\nu} u \frac{\partial T}{\partial x} = \frac{\partial^2 T}{\partial y^2} + \frac{\partial^2 T}{\partial z^2} \tag{3}$$

This differential equation describes the temperature field within the fluid in any cross section of the passages.

The value of the temperature gradient $\frac{\partial T}{\partial x}$ in equation (3) can be connected with the internal heat generation by a heat balance made up for the entire perimeter enclosing one of the fluid passages. For reasons of symmetry, half of the total heat generated within the wall which surrounds one passage is transferred by conduction to the fluid flowing through this passage and increases its temperature in the axial direction:

$$\frac{rsC}{2} = \rho g c \bar{u} A \frac{\partial T}{\partial x} \tag{4}$$

This equation is used to replace the gradient $\frac{\partial T}{\partial x}$ in equation (3).

$$\frac{\partial^2 T}{\partial y^2} + \frac{\partial^2 T}{\partial z^2} = \frac{u}{\bar{u}} \frac{rsC}{2kA} \tag{5}$$

The boundary condition is determined by the fact that all the heat generated by internal heat sources within the passage walls must in steady state be transferred into the coolant. Since, according to assumption 5, the heat conduction within the passage walls can be neglected, this condition applies to any differential length dC along the circumference of the passages (fig. 1). Each passage wall borders on two fluid passages (a and b in fig. 1) and the heat flow transferred by conduction into the coolant on both sides must be equal to the internal heat generation within the wall. This relation is described by the equation

$$rs\, dC = -k \left[\left(\frac{\partial T}{\partial n} \right)_a + \left(\frac{\partial T}{\partial n} \right)_b \right] dC \tag{6}$$

where n denotes the outward normal to the passage wall surface and the two indices a and b refer to the two fluid passages. The internal heat generation r per unit volume is postulated to be constant. Therefore,

$$\left(\frac{\partial T}{\partial n} \right)_a + \left(\frac{\partial T}{\partial n} \right)_b = -\frac{rs}{k} = \text{constant} \tag{7}$$

Equations (5) and (7) describe the temperature field within the coolant.

DIMENSIONLESS VARIABLES

In order to generalize the analysis, by reducing the number of parameters, the equations derived in the previous section are transformed with the aid of the following dimensionless variables:

$$y^* = \frac{y}{D}; \quad z^* = \frac{z}{D}; \quad n^* = \frac{n}{D}; \quad u^* = \frac{u}{\bar{u}}; \quad T^* = T\left(\frac{2k}{rsD}\right)$$

where the hydraulic diameter D is defined as four times the cross-sectional flow area divided by the circumference of the passage. Equations (5) and (7) become

$$\frac{\partial^2 T^*}{\partial y^{*2}} + \frac{\partial^2 T^*}{\partial z^{*2}} = 4u^* \tag{8}$$

and

$$\frac{1}{2}\left[\left(\frac{\partial T^*}{\partial n^*}\right)_a + \left(\frac{\partial T^*}{\partial n^*}\right)_b\right] = -1 \tag{9}$$

Equations (8) and (9) together with a symmetry condition fully determine the problem. A typical symmetry condition is shown in figure 1. Here the normal derivative at point 1 and directed towards passage b is equal to the normal derivative at a similarly located point 2 and directed towards passage a.

The dimensionless velocity u^* is a function of y^*, z^*, and the Reynolds number and expresses the shape of the velocity field in the passage. For noncircular passages the velocity field is known only from Nikuradse's measurements for Reynolds numbers of about 40,000. Experiments with circular tubes have shown, however, that the shape of a turbulent velocity profile changes only slightly with Reynolds number. In addition, the temperature field is not influenced strongly by the velocity field (appendix A). The dependence of u^* on the Reynolds number will therefore be neglected, and the velocity profile will be regarded as a unique function for any specific passage shape. Equations (8) and (9) then have a unique solution for any given passage configuration.

CALCULATION OF TEMPERATURE DISTRIBUTIONS

An analytic solution of equations (8) and (9) can be found only when u^* is a given analytic function of y^* and z^* and when the boundaries of the passages are relatively simple shapes. Neither of these conditions apply to the problem under consideration. The equations are therefore solved numerically by means of the relaxation method. For this purpose they are expressed in finite-difference form.

2164

Consider a grid, or net of points, placed into a cross section of the flow passages as indicated in the following sketch:

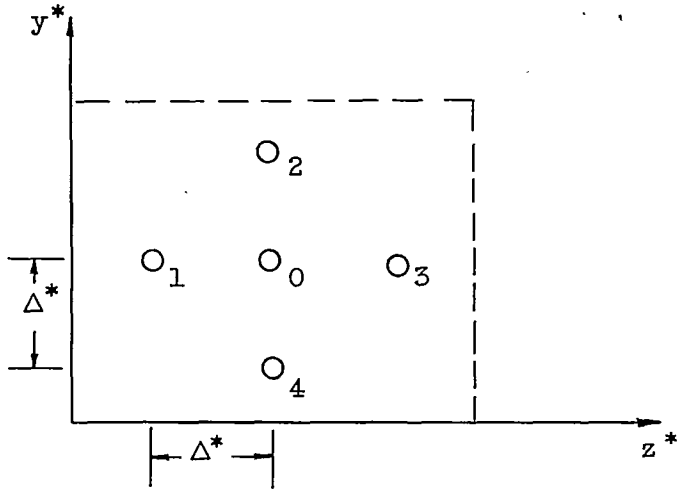

Adjacent points are separated by a small, but finite, distance Δ^*. The derivatives of T^* at a point 0 can be approximated by differences of the temperature at surrounding points. Thus the first derivatives are

$$\left(\frac{\partial T^*}{\partial y^*}\right)_0 \sim \frac{T_4^* - T_0^*}{\Delta^*} \qquad \left(\frac{\partial T^*}{\partial y^*}\right)_2 \sim \frac{T_0^* - T_2^*}{\Delta^*}$$

$$\left(\frac{\partial T^*}{\partial z^*}\right)_0 \sim \frac{T_1^* - T_0^*}{\Delta^*} \qquad \left(\frac{\partial T^*}{\partial z^*}\right)_3 \sim \frac{T_0^* - T_3^*}{\Delta^*}$$

The second derivatives are approximated by differences of the first derivatives and become

$$\frac{\partial^2 T^*}{\partial y^{*2}} \sim \frac{(T_4^*-T_0^*) - (T_0^*-T_2^*)}{\Delta^{*2}} = \frac{T_2^* + T_4^* - 2T_0^*}{\Delta^{*2}}$$

$$\frac{\partial^2 T^*}{\partial z^{*2}} \sim \frac{(T_1^*-T_0^*) - (T_0^*-T_3^*)}{\Delta^{*2}} = \frac{T_1^* + T_3^* - 2T_0^*}{\Delta^{*2}}$$

With these values, equation (8) becomes

$$T_1^* + T_2^* + T_3^* + T_4^* - 4T_0^* - 4u_0^*\Delta^{*2} = 0 \qquad (10)$$

The boundary condition can be expressed in finite-difference form by assuming, for example, that points 1, 0, and 3 lie along a passage wall and points 2 and 4 in two adjacent passages. The normal derivatives are then expressed as differences of the temperature at points 2, 0, and 4. Equation (9) becomes

$$\frac{1}{2}\left[\left(\frac{T_2^*-T_0^*}{\Delta^*}\right) + \left(\frac{T_4^*-T_0^*}{\Delta^*}\right)\right] = -1$$

or

$$T_2^* + T_4^* - 2T_0^* + 2\Delta^* = 0 \qquad (11)$$

In some of the later calculations the wall passes through point 0 at an angle of 45° with respect to the grid. The boundary condition is then expressed as follows:

$$T_1^* + T_2^* + T_3^* + T_4^* - 4T_0^* + 2\sqrt{2}\Delta^* = 0 \qquad (12)$$

Equation (10) together with boundary conditions (11) or (12) was solved by the relaxation method for heat exchangers composed of rectangular and triangular passages. In the case of the triangular passages, the solution is universal, that is, it applies to all heat exchangers with the same passage configuration, regardless of the physical dimension. In the case of the rectangular passages, however, the solution depends on the width-to-height ratio of the passages. Because only one particular solution is presented for the rectangular configuration, the method of solution for this case will be described in detail. The essential features of the relaxation method (see, for example, reference 5) can be outlined as follows:

Suppose it is desired to solve a given finite-difference equation over a certain area of integration. The equation is of the following type:

$$f(T^*) = 0 \tag{13}$$

The solution of this equation must also satisfy prescribed conditions at the boundary of the area of integration.

First, it is necessary to select a net of points covering the entire area of integration. The distance Δ^* between net points is arbitrary, with the accuracy of the final solution increasing as the distance between points is decreased. Next, values of T^* are assumed at each net point. In general, these assumed values of the function will not satisfy the difference equation, and the left-hand side of equation (13) is equal to some residual value N instead of zero. At any given net point, it is then necessary to adjust T^* in order to make N vanish at that point. This adjustment of T^* also changes the residuals at adjacent net points. However, if this process of adjustment is started at the point at which the absolute value of N is greatest, and is then repeated for points at which the value of the residual is successively less, the correct values of T^* for the entire net eventually are obtained.

This method is now applied to a heat exchanger composed of rectangular passages as shown in figure 2. The problem can be simplified by taking advantage of the symmetry of the heat exchanger. Lines AB, AE, and DE are lines of symmetry, and there can be no flow of heat across these lines. Furthermore, the temperature distribution is also centrally symmetric about point C. The temperature distribution need therefore only be found within the area bounded by AEDCB. An enlarged view of this area, showing some of the net points, is presented in figure 3.

The approximate finite-difference equation for all internal points is obtained from equation (10). For point g it is

$$T_f^* + T_c^* + T_h^* + T_k^* - 4T_g^* - 4u_g^*\Delta^{*2} = N_g \tag{14}$$

Point g is the point under consideration, whereas points f, c, h, and k are adjacent points. For points along a line of symmetry within the fluid, as for example point c, the following equation applies.

$$T_b^* + 2T_g^* + T_d^* - 4T_c^* - 4u_c^*\Delta^{*2} = N_c \tag{15}$$

Along wall AB, which is also a line of symmetry, equation (11) becomes (for point e)

$$2T_f^* - 2T_e^* + 2\Delta^* = N_e \tag{16}$$

The following equation is found for point t and similar equations apply for all points along wall BCD

$$T_p^* + T_u^* - 2T_t^* + 2\Delta^* = N_t \tag{17}$$

Finally, the following equation can be derived for the corners of the walls B and D by first writing an equation analogous to equation (17) for points m, x, and q, then eliminating T_m^* with an equation analogous to equation (16) for points n and m, and finally combining the residual values into a single value N_q,

$$T_n^* + T_x^* - 2T_q^* + 3\Delta^* = N_q \tag{18}$$

Before computing the residuals at each net point, it is necessary to assume temperatures and to determine velocities at all points. The velocity distributions u^* for triangular and rectangular passages were obtained from references 2 and 3 and are shown in dimensionless form in figures 4 and 5. The temperature level within any cross section of the passage depends on the distance of that cross section from the passage entrance and all temperatures found will contain an arbitrary additive constant. It is therefore possible to assume arbitrarily the temperature at one point within the configuration. An estimate of all other temperatures can be obtained from the circular tube solution as presented in appendix A or the flat plate solution as presented in appendix B.

Once the temperature distribution has been assumed, it remains to determine the residuals at all net points with equations similar to equations (14) to (18). The point at which N has the largest absolute value is then selected and T^* at that point is adjusted so that the residual vanishes. The effect of this adjustment on the residuals at adjacent points is calculated with the aid of the appropriate finite-difference equation. The process is then carried out for the point at which the next largest residual appears. Eventually, if the process is repeated often enough, the residuals at all net points approach zero, and the final adjusted values of T^* satisfy the approximate equations at all net points.

The accuracy of the solution can be determined by increasing the number of net points. The change in the temperature distribution due to an increase of the number of net points is a measure of the correctness of the solution.

RESULTS

The method outlined in the previous section was applied to heat exchangers composed of a large number of triangular and rectangular passages. In each case the passages were staggered in order to minimize the expected hot spots.

Temperature distribution in triangular passages. - The triangular configuration is represented by figure 1. Each passage in this configuration is an isosceles right triangle. Temperature distributions in the walls of this heat exchanger are presented in figure 6. The ordinate in this figure is the dimensionless wall temperature T_w^* including an additive constant. Temperature distributions found with nets of 28, 49, and 91 grid points are included. From a comparison of these distributions, it can be seen that the maximum error in the final solution (91 points) is less than 5 percent of the maximum temperature difference.

The additive constant in the solution can be eliminated by forming a difference of the local temperature and the bulk temperature of the fluid, where the bulk temperature is given by

$$T_B = \frac{1}{A\bar{u}} \int_A uT \, dA \tag{19}$$

or, in terms of the dimensionless variables

$$T_B^* = \frac{1}{A^*} \int_{A^*} u^* T^* \, dA^* \tag{20}$$

In order to simplify the interpretation of the results of this paper and for purposes of comparison with the results of reference 1, the temperature difference $(T_w^* - T_B^*)$ was divided by a similar temperature difference for a circular tube $(T_w^* - T_B^*)_c$, which is found in appendix A. This temperature-difference ratio for the triangular heat exchanger is presented in figure 7. The use of the dimensional temperatures T instead of the nondimensional values T^* as the ordinate of this figure is justified when the circular tube has the same rate of heat generation, wall thickness, and hydraulic diameter as the noncircular passage. Contours of equal temperature (isotherms) within the coolant of the triangular heat exchanger are shown in figure 8.

Temperature distribution in rectangular passages. - Figure 2 represents the rectangular configuration. The width-to-height ratio of each passage in this configuration is 3.5. The temperature-difference ratio $(T_w-T_B)/(T_w-T_B)_c$ for this heat exchanger is shown in figure 9. The temperature distribution for this case was found with a relaxation net of 79 points. The accuracy of this solution, however, is at least as good as the accuracy of the solution for the triangular heat exchanger, because the dimensionless distance between net points is smaller for the rectangular heat exchanger. Contours of equal temperature within the coolant are shown in figure 10.

The width-to-height ratio of each passage in the rectangular heat exchanger is 3.5. It is to be expected, however, that the temperature distribution near the corners is the same for passages with any ratios greater than 3.5. Proof of this supposition can be found in figure 11, where the temperature profile within the coolant on a normal to the wall at point C (fig. 2) is compared with the profile between two parallel infinite plates (appendix B). It is assumed that the distance d between opposite walls is the same for both solutions. The comparison is unsatisfactory when the temperature difference is based on the bulk temperature of the entire passage, because that particular bulk temperature includes much of the low velocity coolant near the corners. If, however, the temperature difference is based on a local bulk temperature existing at the section of the passage under consideration, (dashed curve) then the agreement is excellent. This agreement shows that the influence of the corners on the flow of heat at a station halfway between the corners is already very small for a width-to-height ratio of only 3.5. Thus, the influence of one corner on the opposite corner is even smaller, which means that the temperature distribution in a corner of the rectangle with the width-to-height ratio of 3.5 does not differ markedly from the temperature field in the corner of a rectangle of any greater ratio.

Influence of velocity field on temperature field. - A certain error may be introduced by the assumption that the velocity profiles measured by Nikuradse apply under all conditions, even in nonisothermal flow. In order to estimate the magnitude of this error, temperature distributions in the circular tube were calculated for both a constant velocity and a 1/7th power velocity profile. Figure 12 shows that the variation in the temperature distribution caused by this extreme change in the velocity profiles is not large. It is therefore believed that a small error in the velocity profiles will cause a negligible error in the temperature distribution in noncircular passages as well.

Comparison with Prandtl number 1 solution. - A comparison of the results presented herein and the results of reference 1 shows that the ratio of the temperature differences in the walls to the difference of the average wall temperature and the bulk temperature in heat exchangers with triangular and rectangular passages is very much greater for a very low Prandtl number than for a Prandtl number near 1. The dimensionless temperature difference $(T_w^*-T_B^*)_c$ for a circular tube and a coolant with a very low Prandtl number is 0.146 (appendix A). The corresponding temperature difference for a coolant with $Pr = 1$ is given by equation (31) of reference 1:

$$(T_w^*-T_B^*)_c = \frac{1}{2}\frac{k^*s^*}{Nu}$$

The dimensionless temperature differences in noncircular tubes can be compared for $Pr << 1$ and $Pr = 1$ by multiplying the temperature-difference ratios by the appropriate circular tube value. The dimensional temperature differences follow from the definitions of T^*. It has to be kept in mind, however, that these definitions differ in the two reports, and that T^* as used in the present report is based on the thermal conductivity of the coolant, whereas in reference 1, T^* is based on the thermal conductivity of the wall material.

A first approximation of the temperature distribution in the walls of heat exchangers cooled by fluids with a Prandtl number between 0 and 1 might be obtained by a linear interpolation of the results of the present report and the results of reference 1.

CONCLUSIONS

A method to calculate the temperature distribution in a heat exchanger composed of noncircular flow passages and cooled by a fluid with a Prandtl number much lower than 1 has been presented.

The differential equations describing the flow of heat were written in terms of dimensionless variables, so that their solution becomes a function only of the geometry of the heat exchanger. The equations were then solved for heat exchangers with triangular and rectangular passages. In the case of triangular passages, the solution is universal and applies to all similar heat-exchanger configurations composed of isosceles right triangles. In the case of rectangular passages, the solution is a function of the width-to-height ratio of each passage. Results for the rectangular heat exchanger were presented only for a width-to-height ratio of 3.5, but it was shown that these results can be generalized to include passages with any ratio greater than 3.5.

Temperature differences in the walls and within the coolant of these heat exchangers were evaluated numerically. The evaluations show a pronounced temperature increase near the corners of the passages.

A comparison of the ratio of the temperature differences within the wall to the difference of the average wall temperature and the coolant bulk temperature of heat exchangers cooled with a fluid having a very low Prandtl number and of the same temperature-difference ratio for similar heat exchangers cooled with a fluid having a Prandtl number of 1 shows that the temperature-difference ratios for the low Prandtl number are much greater than those for a Prandtl number of 1.

Lewis Flight Propulsion Laboratory,
National Advisory Committee for Aeronautics,
Cleveland, Ohio, April 10, 1951.

APPENDIX A

TEMPERATURE DISTRIBUTION IN CIRCULAR TUBES

The transformation of equation (8) into a cylindrical coordinate system with rotational symmetry results in:

$$\frac{1}{R^*}\frac{dT^*}{dR^*} + \frac{d^2T^*}{dR^{*2}} = 4u^* \tag{A1}$$

If it is assumed that half the heat generated flows into the tube whereas the other half flows in an outward direction, then equation (9) becomes

$$\left(\frac{dT^*}{dR^*}\right)_{R^* = 1/2} = 1 \tag{A2}$$

Equation (A1) together with boundary condition (A2) can be solved provided that u^* is a known function of R^*. A simple solution can be obtained by making the assumption that u^* is a constant and equal to 1. The solution of equation (A1) satisfying (A2) is

$$T^* = R^{*2} + C_1 \tag{A3}$$

where C_1 is an arbitrary constant. The bulk temperature as defined in equation (20) becomes

$$T_B^* = 0.125 + C_1 \tag{A4}$$

The temperature difference in a circular tube under the assumption of a constant velocity, therefore, is expressed as follows

$$T^* - T_B^* = R^{*2} - 0.125 \tag{A5}$$

A solution more representative of the problem can be obtained by assuming that the velocity varies as the 1/7th power of (1-R)

$$\frac{u}{u_m} = \left(1 - \frac{2R}{D}\right)^{1/7}$$

or, in the dimensionless system of coordinates:

$$u^* = \frac{60}{49}(1-2R^*)^{1/7} \tag{A6}$$

With this assumption the solution of equation (A1) becomes

$$T^* = \frac{1}{2}\left[\ln (2R^*) + (1-2R^*)^{15/7} + \sum_{p=1}^{\infty} \frac{(1-2R^*)^{(p+15/7)}}{p+15/7}\right] + C_1$$

$$0 < R^* \leq \frac{1}{2} \tag{A7}$$

Equation (A7) has a logarithimic singularity at $R^*=0$. A solution of equation (A1) at $R^*=0$ exists, however. This solution is:

$$T^* = -\frac{41}{240} - \frac{1}{2}\sum_{p=1}^{\infty} \frac{1}{p(7p+1)} + C_1 \tag{A8}$$

The bulk temperature is obtained by multiplying equation (A7) by u^* and integrating each term of the equation. The final solution is

$$T_B^* = -0.146 + C_1 \tag{A9}$$

A temperature-difference profile is obtained by subtracting equation (A9) from equations (A7) and (A8). This profile is plotted in figure 12, together with a similar profile as represented by equation (A5).

APPENDIX B

TEMPERATURE DISTRIBUTION BETWEEN TWO PARALLEL INFINITE PLATES

The following equations describe the flow of heat between parallel plates, extending to infinity in the z-direction and separated by a distance d

$$\frac{d^2T^*}{dy^{*2}} = 4u^* \tag{B1}$$

$$\left(\frac{dT^*}{dy^*}\right)_{y^*=0} = -1 \tag{B2}$$

$$D = 2d \tag{B3}$$

A solution of this system of equations can be obtained if u^* is a known function of y^*. The assumption of a 1/7th power profile leads to the following expression

$$\frac{u}{u_m} = \left(2\,\frac{y}{d}\right)^{1/7}$$

or

$$u^* = \frac{8}{7}\,(4y^*)^{1/7} \tag{B4}$$

The temperature distribution is then found to be

$$T^* = \frac{7}{60}\,(4y^*)^{15/7} - y^* + C_1 \tag{B5}$$

The bulk temperature, which is defined by equation (20), becomes

$$T_B^* = -\frac{32}{345} + C_1 \tag{B6}$$

Thus, the temperature-difference parameter for the parallel flat plates is

$$T^* - T_B^* = \frac{7}{60}\,(4y^*)^{15/7} - y^* + \frac{32}{345} \qquad 0 \le y^* \le 1/4 \tag{B7}$$

REFERENCES

1. Eckert, E. R. G., and Low, George M.: Temperature Distribution in Internally Heated Walls of Heat Exchangers Composed of Noncircular Flow Passages. NACA TN 2257, 1951.

2. Nikuradse, J.: Untersuchungen über turbulente Strömungen in nicht kreisförmigen Rohren. Ingenieur-Archiv, Bd. 1, 1930, S. 306-332.

3. Nikuradse, J.: Geschwindigkeitsverteilung in turbulenten Strömungen. VDI Zeitschr., Bd. 70, Nr. 37, Sept. 11, 1926, S. 1229-1230.

4. Eckert, E. R. G.: Introduction to the Transfer of Heat and Mass. McGraw-Hill Book Co., Inc., 1950, pp. 103, 115.

5. Emmons, H. W.: The Numerical Solution of Heat-Conduction Problems. A.S.M.E. Trans., vol. 65, no. 6, Aug. 1943, pp. 607-612.

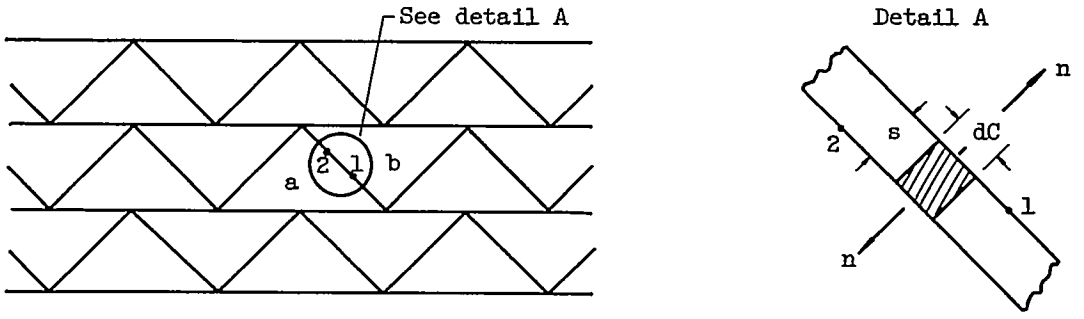

Figure 1. - Cross section through typical heat exchanger composed of triangular passages.

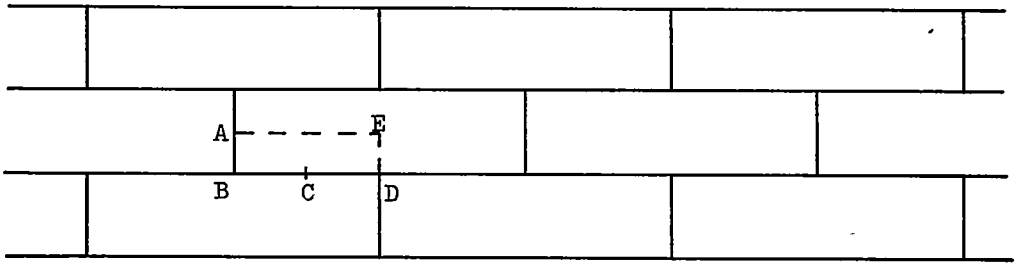

Figure 2. - Cross section through typical heat exchanger composed of rectangular passages.

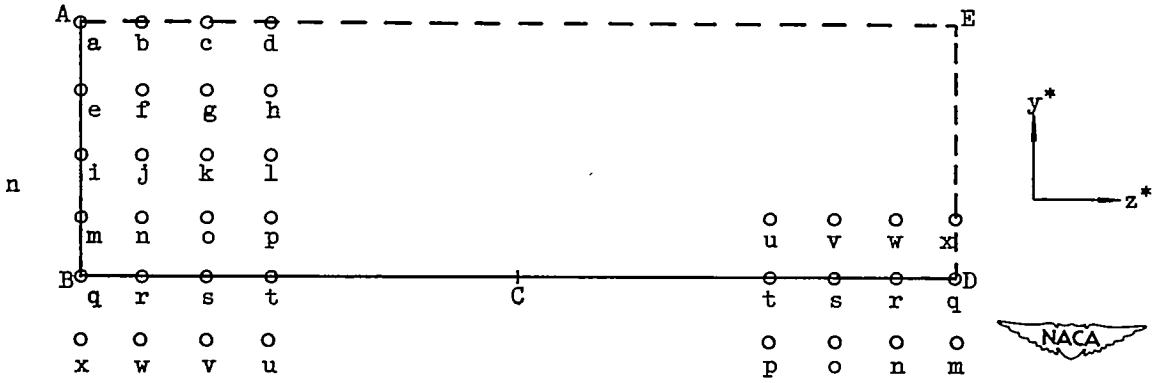

Figure 3. - Relaxation net for rectangular heat exchanger.

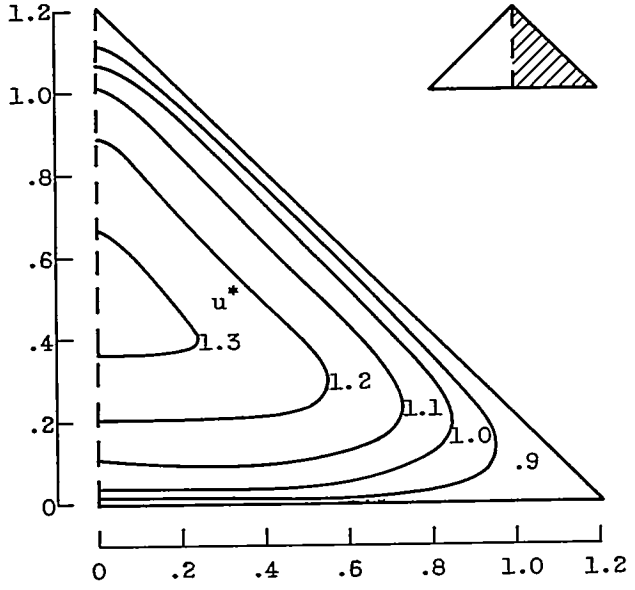

Figure 4. - Velocity contours in triangular passage as measured in reference 2.

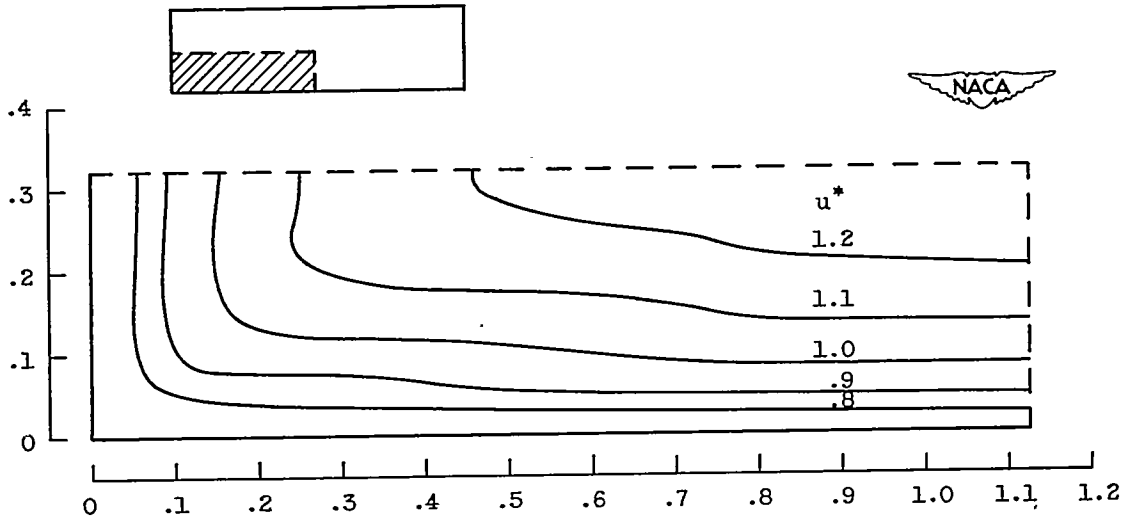

Figure 5. - Velocity contours in rectangular passage as measured in reference 3.

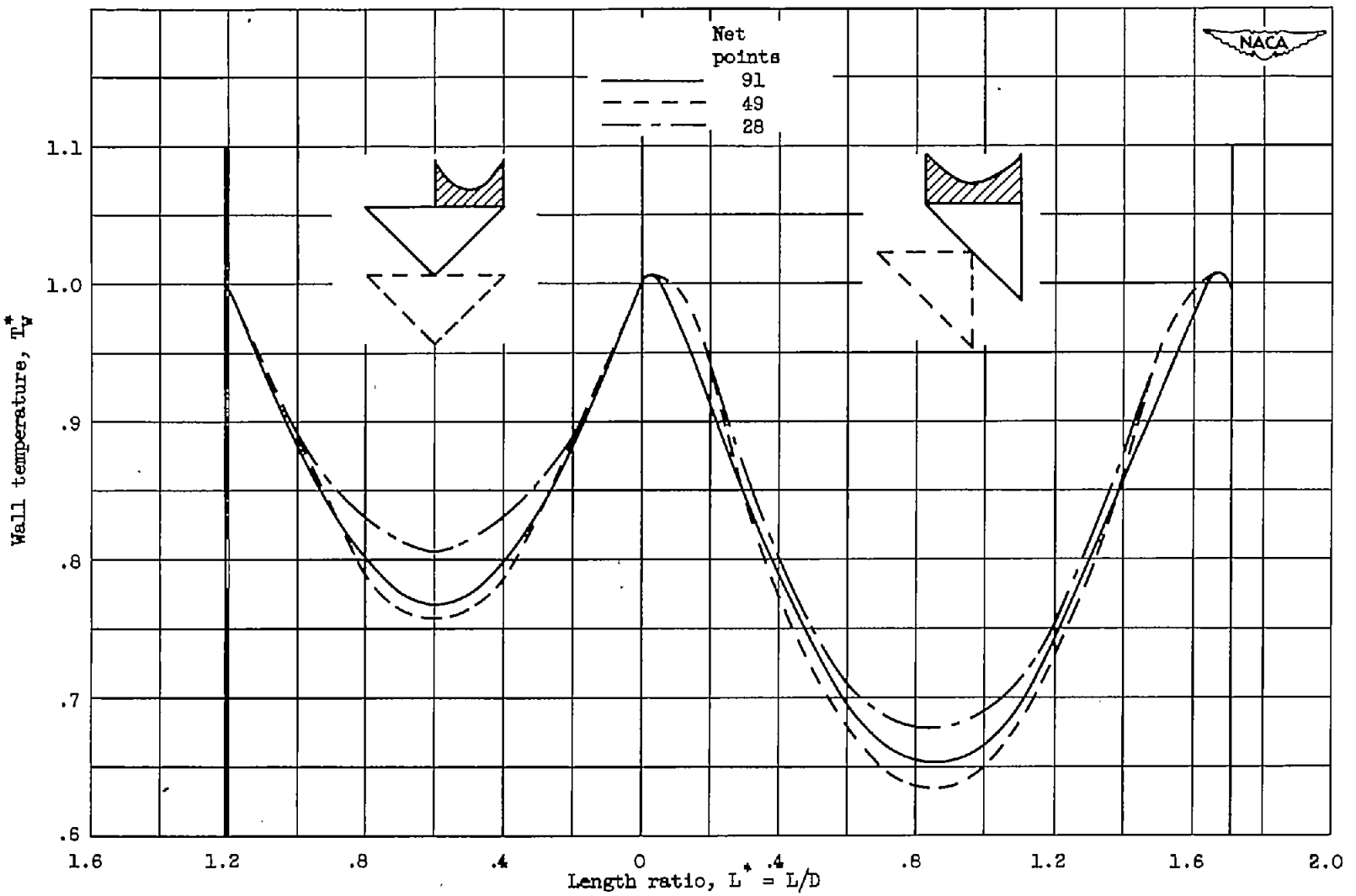

Figure 6. - Comparison of temperature distributions using different number of net points. Triangular heat exchanger.

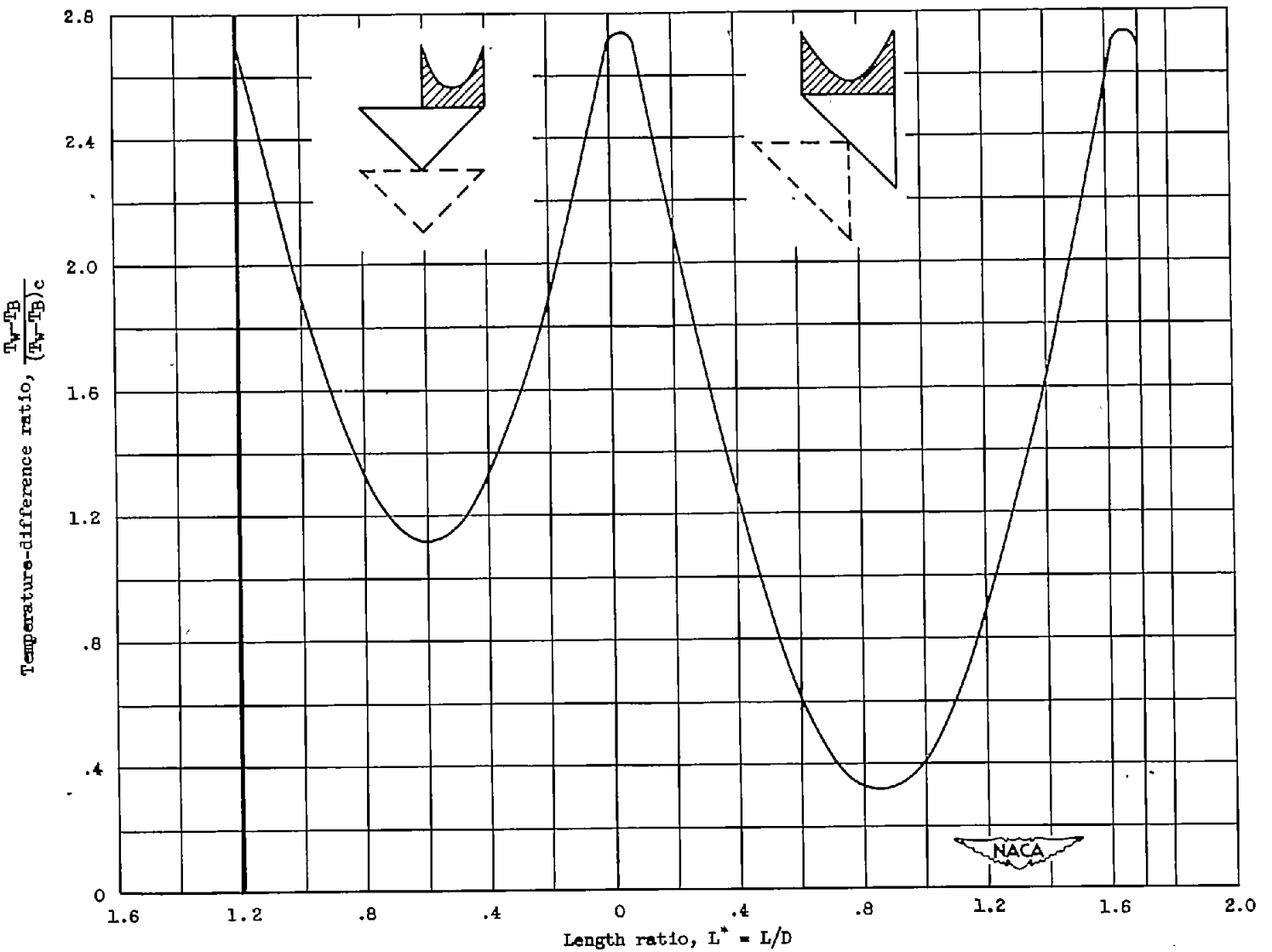

Figure 7. - Wall temperature distribution for passage of triangular heat exchanger.

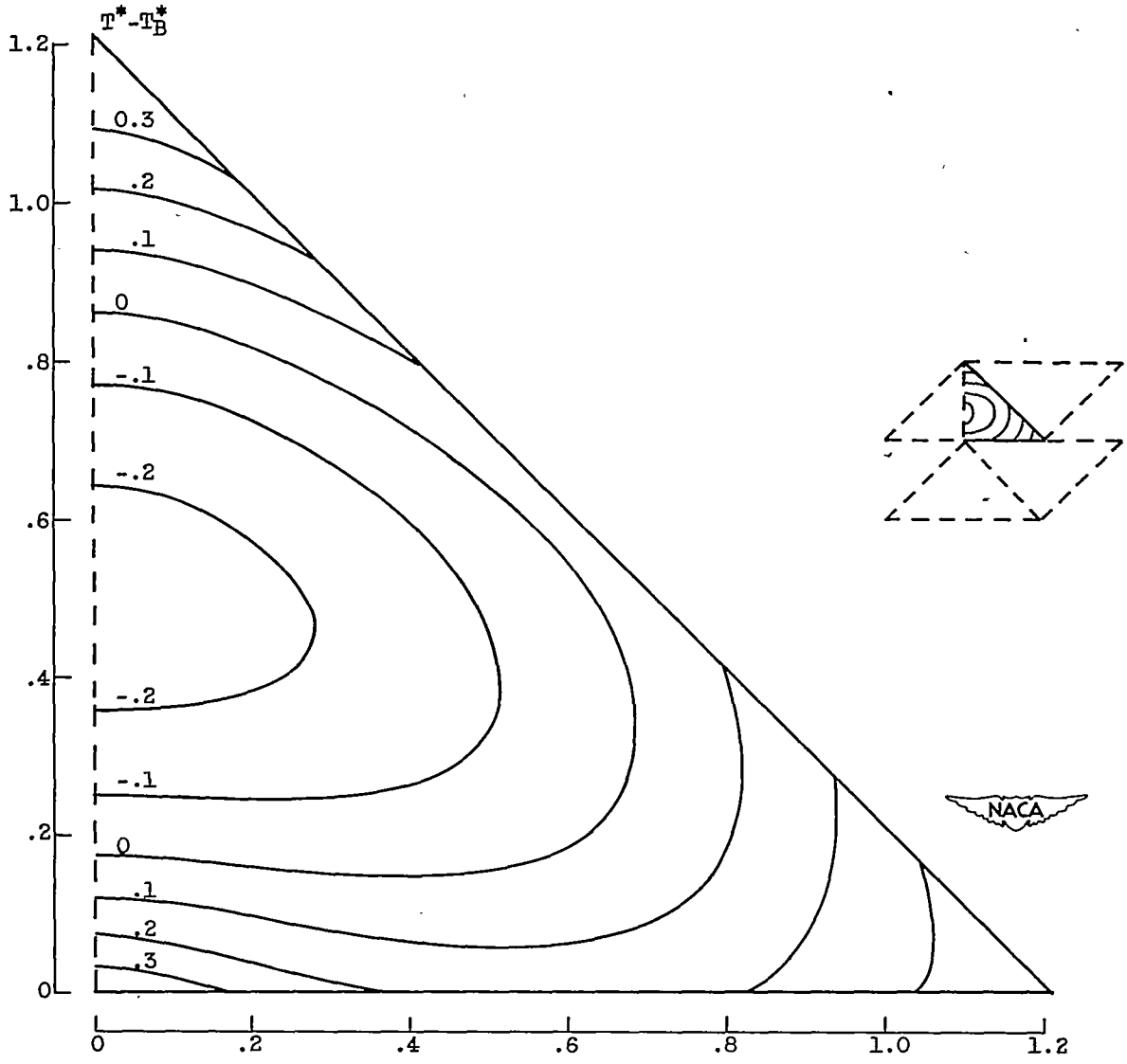

Figure 8. - Temperature of coolant within passage of triangular heat exchanger.

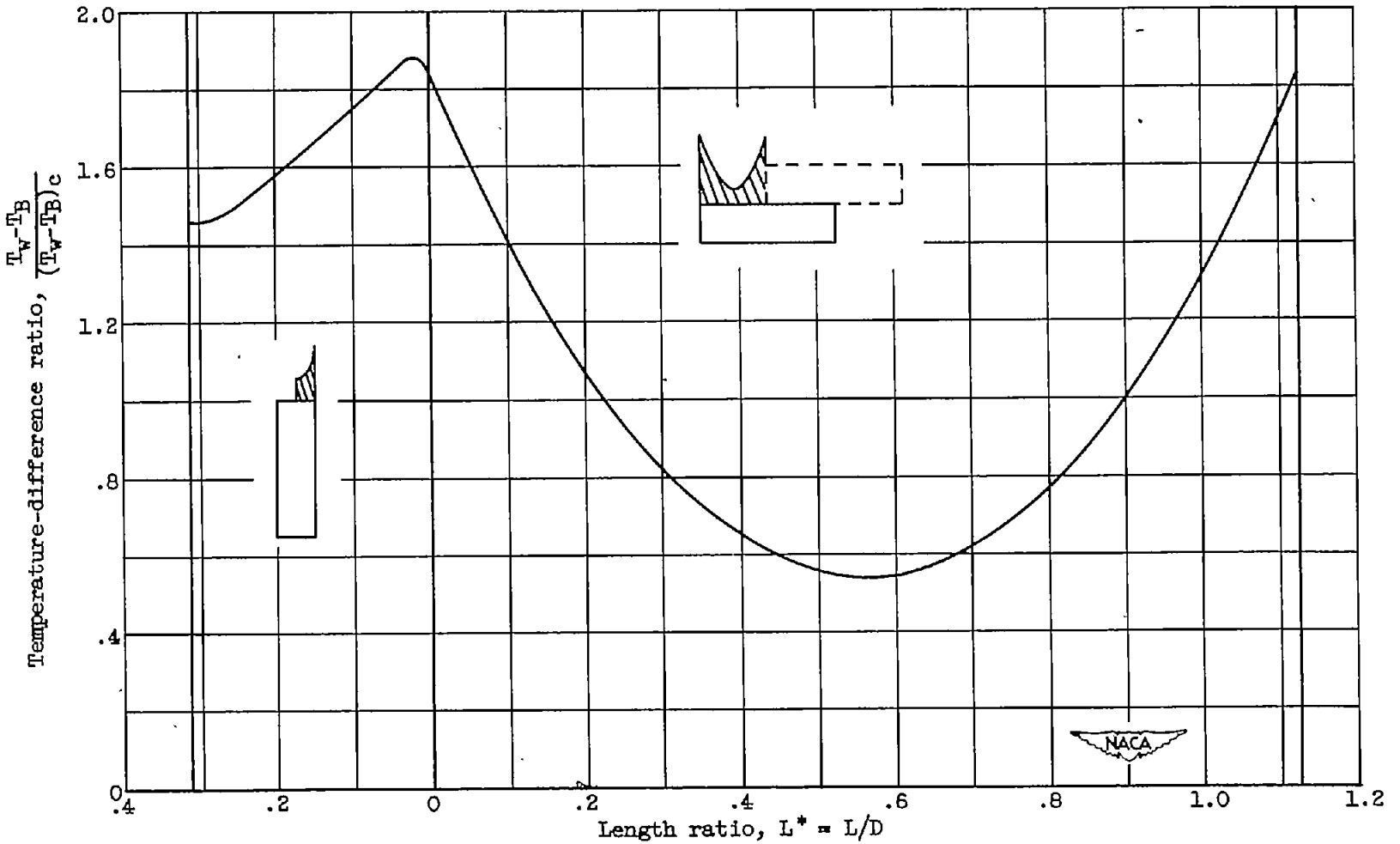

Figure 9. - Wall temperature distribution for passage of rectangular heat exchanger.

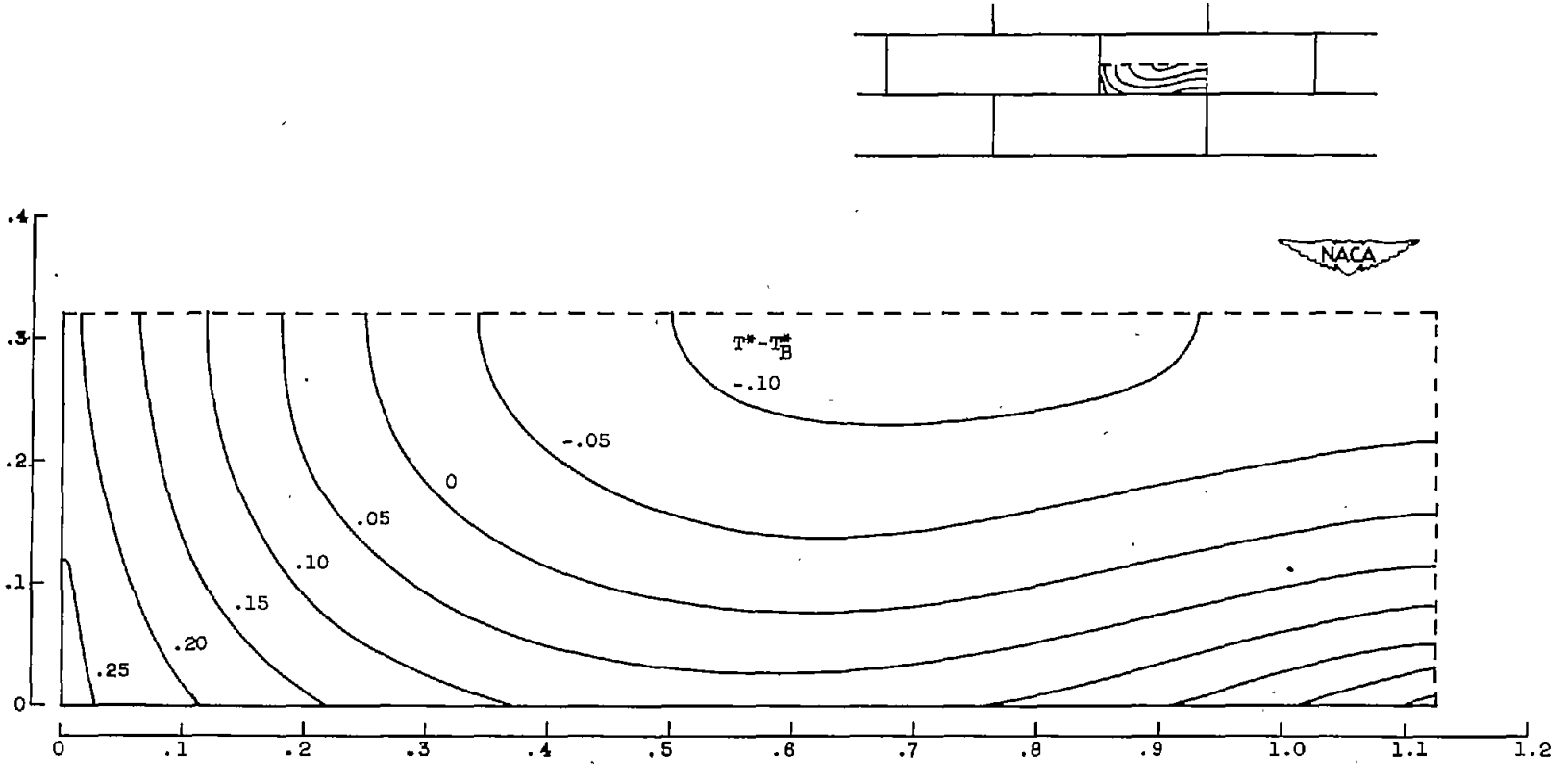

Figure 10. - Temperature of coolant within passage of rectangular heat exchanger.

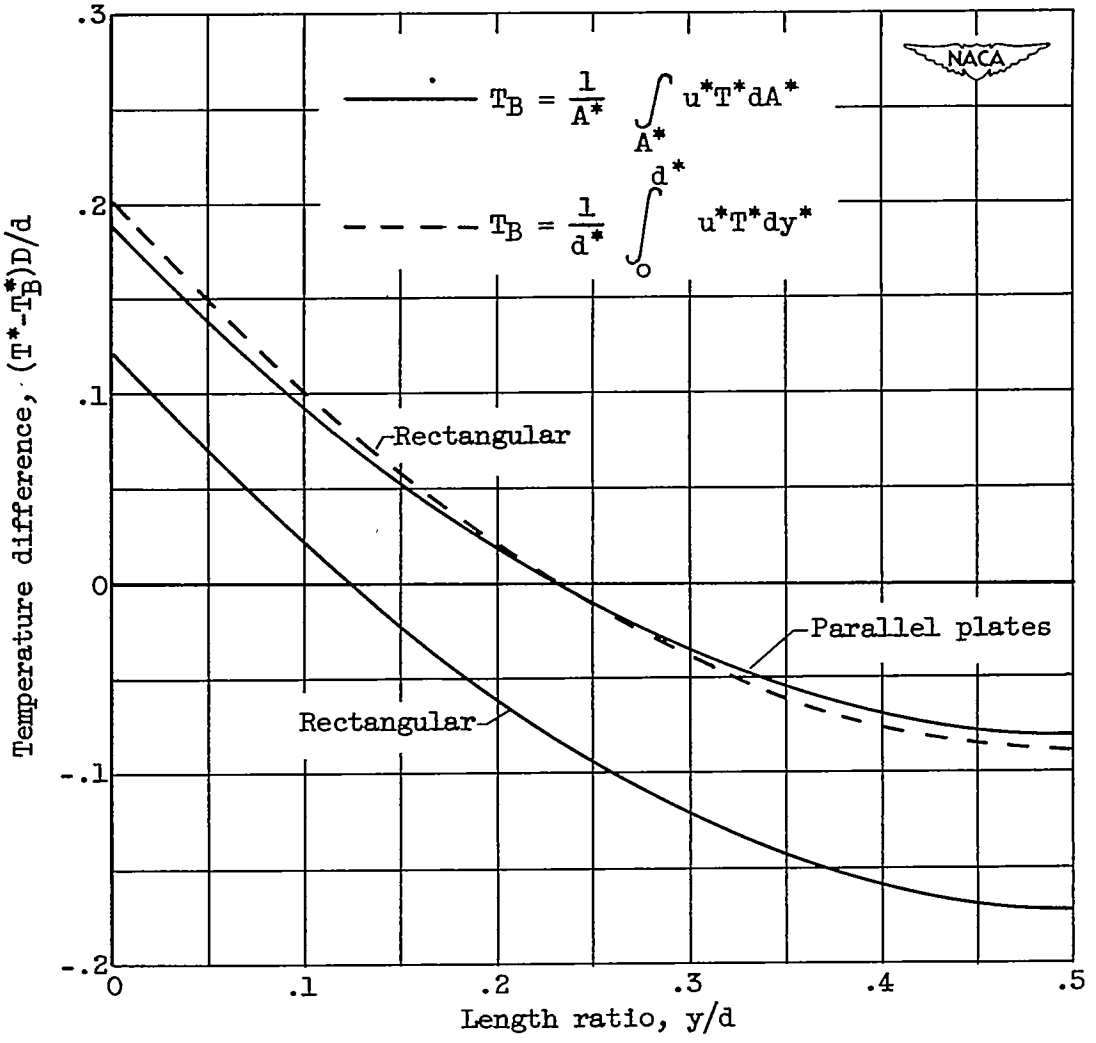

Figure 11. - Temperature distribution within coolant for rectangular configuration at point C (fig. 2) and for two parallel plates.

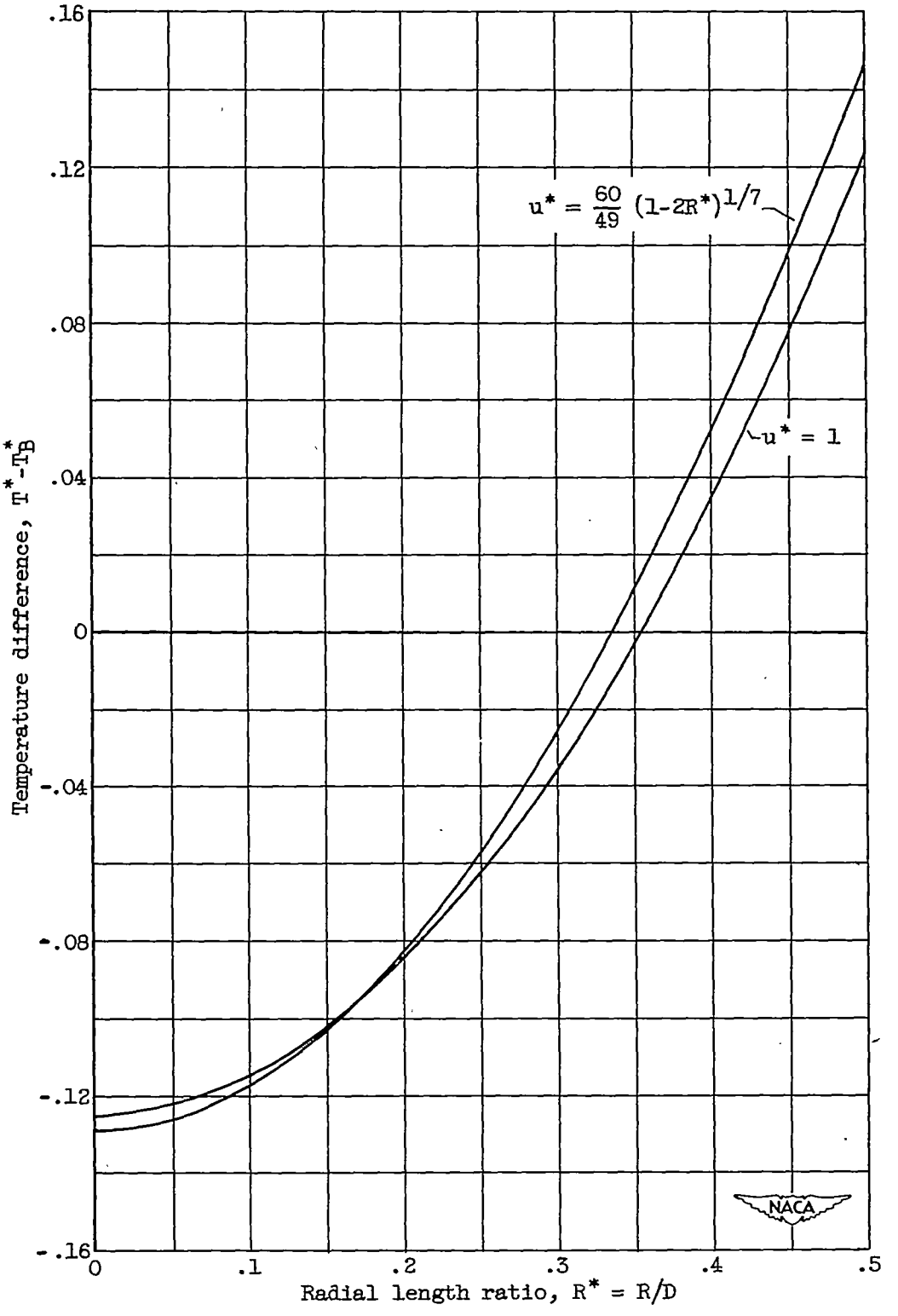

Figure 12. - Temperature distribution in circular tube.

NACA-Langley - 7-2-51 - 1000